

On the Self-Aggregation and Fluorescence Quenching Aptitude of Surfactant Ionic Liquids

Marijana Blesic,^{†,‡} António Lopes,^{*,†} Eurico Melo,[†] Zeljko Petrovski,[§] Natalia V. Plechkova,[‡] José N. Canongia Lopes,^{†,⊥} Kenneth R. Seddon,^{†,‡} and Luís Paulo N. Rebelo^{*,†}

Instituto de Tecnologia Química e Biológica, ITQB 2, Universidade Nova de Lisboa, Apartado 127, 2780-901 Oeiras, Portugal, The QUILL Centre, The Queen's University of Belfast, Stranmillis Road, Belfast BT9 5AG, U.K., and CQFM, Departamento de Engenharia Química e Biológica and Centro de Química Estrutural, Instituto Superior Técnico, 1049-001 Lisboa, Portugal

Received: March 12, 2008

The aggregation behavior in aqueous solution of a number of ionic liquids was investigated at ambient conditions by using three techniques: fluorescence, interfacial tension, and ¹H NMR spectroscopy. For the first time, the fluorescence quenching effect has been used for the determination of critical micelle concentrations. This study focuses on the following ionic liquids: [C_nmpy]Cl (1-alkyl-3-methylpyridinium chlorides) with different linear alkyl chain lengths (*n* = 4, 10, 12, 14, 16, or 18), [C₁₂mpip]Br (1-dodecyl-1-methylpiperidinium bromide), [C₁₂mpy]Br (1-dodecyl-3-methylpyridinium bromide), and [C₁₂mpyr]Br (1-dodecyl-1-methylpyrrolidinium bromide). Both the influence of the alkyl side-chain length and the type of ring in the cation (head) on the CMC were investigated. A comparison of the self-aggregation behavior of ionic liquids based on 1-alkyl-3-methylpyridinium and 1-alkyl-3-methylpyridinium cations is provided. It was observed that 1-alkyl-3-methylpyridinium ionic liquids could be used as quenchers for some fluorescence probes (fluorophores). As a consequence, a simple and convenient method to probe early evidence of aggregate formation was established.

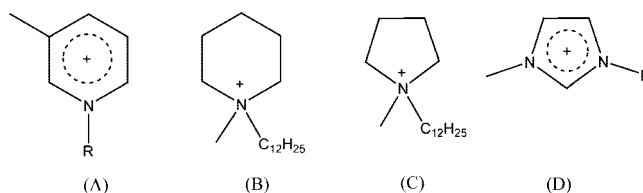
1. Introduction

Considering the growing number of reported investigations in which the dual nature of ionic liquids¹ has been studied, it seems that their roles in both surfactant science and its applications are promising. Surveying the recent literature, three possible directions for the development and applications of ionic liquids can be identified:

In the first group of publications, the amphiphilic nature of some cations, for example, [C_nmim]⁺, leading to aggregation phenomena in aqueous solutions (and in some cases to organization into micelles displaying surfactant behavior) was analyzed.^{2–14} With the possibility of the fine-tuning of the ionic liquids' hydrophobicity by changing the alkyl chain length and/or the nature and size of the counterion (anion), one can affect both the structure and the delicate dynamics of these micellar aggregates. Second, impressive solvation abilities toward the dissolution of a series of different common surfactants,^{15,16} amphiphilic polymers¹⁷ or ionic liquids^{18,19} in neat ionic liquids have been demonstrated. Third, ionic liquids can be added as a cosurfactant or hydrotrope to aqueous solutions of common surfactants, thus affecting the surface activity and the critical micelle concentration (CMC) of these solutions.^{3,6}

In our previous work,³ we reported the role of the alkyl chain length, the concentration, and the nature of the anion on the aggregation behavior of the ionic compounds belonging to the [C_nmim]X (X = Cl, [PF₆] or [NTf₂]) family. In the current contribution, we also examine the influence of different cationic

SCHEME 1: Cations of Ionic Liquids Discussed: (A) 1-Alkyl-3-methylpyridinium, [C_nmpy]⁺; (B) 1-Methyl-1-dodecylpiperidinium, [C₁₂mpip]⁺; (C) 1-Methyl-1-dodecylpyrrolidinium, [C₁₂mpyr]⁺; (D) 1-Alkyl-3-methylimidazolium, [C_nmim]⁺



ring types on the aggregation behavior by using aqueous solutions of [C₁₂Y]Br (Y = mpyrr, mpy, or mpip).

Recently, a few studies on the fluorescence behavior of imidazolium and pyrrolidinium ionic liquids were published.²⁰ Here, we show a unique characteristic of some ionic liquids, namely, in the case of the 1-alkyl-3-methylpyridinium family: besides their ability to act as surfactants, they present also a quencher aptitude for the most commonly used fluorescence probes for micellar characterization (fluorophores). Probably, this characteristic has its origin at the pyridinium ring (head), for it is known that other pyridinium-containing cations can also act as quenchers.

2. Experimental Section

Ionic Liquids. The 1-alkyl-3-methylpyridinium chlorides, [C_nmpy]Cl (*n* = 4, 10, 12, 14, 16, or 18), 1-dodecyl-1-methylpyrrolidinium bromide, 1-dodecyl-3-methylpyridinium bromide, and 1-dodecyl-1-methylpiperidinium bromide {[C₁₂Y]Br; Y = mpyrr, mpy, or mpip; see Scheme 1) were synthesized by the reaction of one mole equivalent of the amine 3-methylpyridine, 1-methylpyrrolidine, or 1-methylpiperidine

* Corresponding authors. E-mail: luis.rebelo@itqb.unl.pt and alopes@itqb.unl.pt.

[†] Universidade Nova de Lisboa.

[‡] The Queen's University of Belfast.

[§] Departamento de Engenharia Química e Biológica, Instituto Superior Técnico.

[⊥] Centro de Química Estrutural, Instituto Superior Técnico.

with an excess of the appropriate haloalkane (1.3 mol equivalents). This excess also allows for the reactants to be stirred without additional solvent at 70 °C; the progress of reactions was monitored by ^1H NMR spectroscopy in CDCl_3 . Upon completion of the reaction, there was no evidence for the presence of unreacted amine. The ionic liquids were purified with ethyl ethanoate. The volume of ethyl ethanoate used for the recrystallization was approximately half that of the halide salt. The ethyl ethanoate was decanted, followed by the addition of fresh ethyl ethanoate, and this step was repeated five times. The remaining ethyl ethanoate was removed in vacuo, and the ionic liquids were dried in vacuo (0.1 Pa) to remove any small traces of volatile compounds at moderate temperatures (60–80 °C) for typically 72 h. The detailed syntheses and spectroscopic (NMR, MS) and thermophysical (DSC, TGA) characterization will be reported elsewhere.²¹ All chemicals were purchased from Sigma-Aldrich; the more volatile liquids were purified by distillation under vacuum before use. For the NMR experiments, d^1 -trichloromethane ($\text{D}+0.03\%$, Euriso-top) was used: ^1H - and ^{13}C NMR analyses showed no major impurities in the ionic liquids as prepared above by using a Bruker Avance spectrometer DPX 300.

Chemicals for IFT, Fluorescence, and NMR Measurements. Doubly distilled deionized water was obtained from a Millipore Milli-Q water purification system (Millipore). Both for the interfacial tension (IFT) and fluorescence measurements, $[\text{C}_n\text{mpy}]\text{Cl}$ stock solutions were prepared in either 1.74×10^{-6} M pyrene or slightly less than saturated anthracene aqueous solution, and all studied solutions were prepared from the stock solutions, diluting with the same pyrene or anthracene aqueous solution. Pyrene (Fluka, Germany, 99%) was recrystallized from benzene. Anthracene (Fluka, Germany, *puriss*, for scintillation) and ethanenitrile (Merck, Germany, gradient grade) were used without further purification. For the NMR experiments, D_2O (Cambridge Isotope Laboratory, Andover, MA, D, 99.9%) was used.

Details about the experimental techniques and instrumentation for IFT, fluorescence, and ^1H NMR spectroscopy are found in the Supporting Information.

Ab Initio Calculations. The molecular geometry and charge distribution of isolated 1,1-dimethylpyrrolidinium and 1,1-dimethylpiperidinium cations were obtained by quantum chemical (*ab initio*) calculations. These were performed by using the Gaussian 03 program²² at the HF/6-31G(d) level of theory for geometry optimization and the MP2/cc-pVTZ-f level for single-point energy and electronic density calculations, as is current practice in the development of force-field parameters for ions present in ionic liquids.²³ The point-charge assignment was done by using the CHelpG algorithm.

3. Results and Discussion

Self-Aggregation Assessment by Surface Tension. The surface tension of aqueous solutions of 1-alkyl-3-methylpyridinium chlorides, $[\text{C}_n\text{mpy}]\text{Cl}$, ($n = 10, 12, 14, 16$, or 18) was measured, see Figure 1a. The results of the IFT for the aqueous solutions as a function of the total concentration of $[\text{C}_n\text{mpy}]\text{Cl}$ were used to determine the CMC and to study adsorption parameters: the efficiency of adsorption, pC_{20} , (defined as the negative logarithm to the base 10 of the concentration of amphiphilic molecules required to reduce the surface tension of the pure solvent by 20 mN m^{-1}), the effectiveness of the surface tension reduction, Π_{CMC} , (defined as $\Pi_{\text{CMC}} = \gamma_0 - \gamma_{\text{CMC}}$, where γ_0 is surface tension of the pure solvent (water) and γ_{CMC} the surface tension of the solution

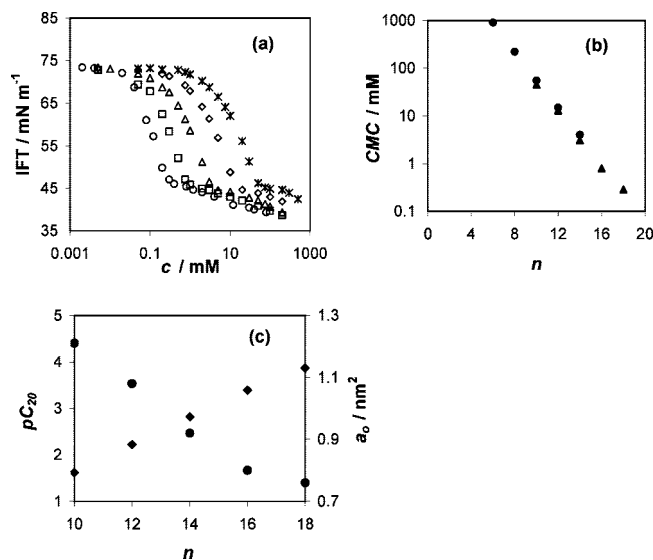


Figure 1. (a) Monitoring the self-aggregation of $[\text{C}_n\text{mpy}]\text{Cl}$ by using IFT for different chain lengths: $n = (*)10, (\diamond)12, (\Delta)14, (\square)16, (\circ)18$. (b) CMC values for $[\text{C}_n\text{mpy}]\text{Cl}$ (\blacktriangle) and $[\text{C}_n\text{mim}]\text{Cl}$ (\bullet) as a function of n . (c) Efficiency of adsorption pC_{20} (\blacklozenge) and minimum area per ionic liquid molecule, a_0 (\bullet) as a function of n $[\text{C}_n\text{mpy}]\text{Cl}$.

TABLE 1: CMC (in mM) of $[\text{C}_n\text{mpy}]\text{Cl}$ ($n = 10$ – 18), $[\text{C}_{12}\text{Y}]\text{Br}$, ($\text{Y} = \text{mpyrr}$, mpy , mpip , and mim) Measured by IFT, Fluorescence Quenching of Pyrene, Fluor, and ^1H NMR Spectroscopy^a

Ionic Liquid	IFT	fluor	^1H NMR
$[\text{C}_{10}\text{mpy}]\text{Cl}$	45	44 ^b	
$[\text{C}_{12}\text{mpy}]\text{Cl}$	13	13.5	12.5
$[\text{C}_{14}\text{mpy}]\text{Cl}$	3.1	3.1	3.2
$[\text{C}_{16}\text{mpy}]\text{Cl}$	0.8	0.77	0.9
$[\text{C}_{18}\text{mpy}]\text{Cl}$	0.3	0.23	0.25
$[\text{C}_{12}\text{mpy}]\text{Br}$	10		
$[\text{C}_{12}\text{mpip}]\text{Br}$	11		
$[\text{C}_{12}\text{mpyrr}]\text{Br}$	1.2		
$[\text{C}_{12}\text{mim}]\text{Br}$	9, 10, 12 ^c , 9.8 ^d		

^a The experimental errors for all used techniques are $\leq 5\%$.

^b Result obtained by using anthracene as a fluorophore. ^c From ref 9. CMCs obtained by using conductivity, volume, and fluorescence measurements. ^d From ref 7. CMC obtained by using conductivity measurements.

at the CMC), and the minimum area per amphiphilic molecule at the interface, a_0 .²⁴

Micellisation. If aggregation phenomena occur, then, as the concentration of an ionic liquid increases, the surface tension of the solution initially decreases and then becomes almost constant. The CMC is determined as the intersection of two linearly extrapolated lines. It is obvious that the decrease in the CMC of aqueous solutions of $[\text{C}_n\text{mpy}]\text{Cl}$ is a consequence of the growth of the alkyl chain. The experimental values for the break points in the IFT measurement are presented in Table 1 (along with other CMC results from different techniques). Figure 1b summarizes the CMC values obtained with the IFT methodology plotted as a function of the number of carbon atoms, n , in the cationic side chain of $[\text{C}_n\text{mpy}]\text{Cl}$, $n = 10$ – 18 . For comparison purposes, data obtained for the $[\text{C}_n\text{mim}]\text{Cl}$ family with similar hydrocarbon chain lengths are depicted.³ The expected slightly higher hydrophobicity of the $[\text{C}_n\text{mpy}]$ cation in comparison with the $[\text{C}_n\text{mim}]$ cation is probably the reason for the lower CMC values of the former.

Adsorption. The lowering of the surface tension values, γ , is a consequence of the increased concentration of the ionic

TABLE 2: Efficiency of Adsorption, pC_{20} , Effectiveness of Surface Tension Reduction, Π_{CMC} , and Minimum Area per Ionic Liquid Molecule at the Interface Air/Liquid, a_o of $[C_n\text{mpy}]\text{Cl}$ ($n = 10\text{--}18$)

ionic liquid	pC_{20}	$\Pi_{CMC}/\text{mN m}^{-1}$	a_o/nm^2
$[C_{10}\text{mpy}]\text{Cl}$	1.62	27.9	1.21
$[C_{12}\text{mpy}]\text{Cl}$	2.22	27.9	1.08
$[C_{14}\text{mpy}]\text{Cl}$	2.82	28.0	0.92
$[C_{16}\text{mpy}]\text{Cl}$	3.39	27.9	0.80
$[C_{18}\text{mpy}]\text{Cl}$	3.87	27.8	0.76

liquid at the air–water surface. Because of the almost invariant condition of the surface for concentrations greater than that of the CMC, the chemical potential of the ionic liquid changes only slightly.²⁵ Although the adsorption efficiency, pC_{20} , increases with increasing alkyl chain length (Figure 1c), the effectiveness of the surface tension reduction, Π_{CMC} , varies only slightly. They follow tendencies published for both $[C_n\text{mim}]\text{Cl}$ ¹³ and classical cationic surfactants.²⁴

From surface tension data, by assuming for these low-concentration regimes a monolayer structure at the surface, we calculated the minimum area per ionic liquid molecule, a_o , by using the well-known Gibbs equation.²⁴ Values for a_o , pC_{20} , and Π_{CMC} are listed in Table 2. The dependence of the minimum area per amphiphilic molecule versus the number of carbon atoms in the alkyl chain, n (up to 16 carbon atoms), for $[C_n\text{mpy}]\text{Cl}$ is linear and can be described by $a_o = 1.906 - 0.0695n$ (Figure 1c). A similar dependence for $[C_n\text{mim}]\text{Cl}$ was recently reported,¹³ and the corresponding equation is $a_o = 1.461 - 0.062n$. A comparison of the equations for these two families suggests a higher degree of packing of adsorbed $[C_n\text{mim}]\text{Cl}$ molecules. A slightly lower surface tension in the plateau region reported in our previous paper³ for $[C_n\text{mim}]\text{Cl}$ in comparison with $[C_n\text{mpy}]\text{Cl}$ (Figure 1a) also leads to the same conclusion.

It is well-known that surface tension measurements are a very sensitive test for the presence of impurities, usually being unreacted surface active compounds (long chain chloroalkane in the case of chloride-based ionic liquids that are usually used in excess during the synthesis). The absence of a minimum²⁴ around the CMC confirms the high purity of the ionic liquids used in this study.

CMC Determination by Changes in the Fluorescence of Added Probes. A widely used method for the determination of the aggregation of amphiphilic molecules (surfactants, polymers, and so forth) is the comparison of the intensities of the first, I1, and third, I3, vibronic bands of the pyrene emission spectrum. The ratio I3/I1 is a function of the polarity of the pyrene environment, and it increases with decreasing solvent polarity.^{26,27}

Obviously, the method cannot be applied when the fluorescence of pyrene is quenched by the surfactant itself. This is found to be the case for the 1-alkyl-3-methylpyridinium ionic liquids, in analogy with other cases containing the same common pyridinium ring (head).²⁸ In fact, it was witnessed that the fluorescence of both pyrene and anthracene in water vanished (indistinguishable from the noise level) for all $[C_n\text{mpy}]\text{Cl}$ ionic liquids used in this study, at concentrations for which aggregation is expected. Therefore, it seems that once in the aggregate, the close contact between the fluorophore probe and the 1-alkyl-3-methylpyridinium group results in an efficient static fluorescence quenching. In order to verify that the 1-alkyl-3-methylpyridinium group is able to quench the fluorescence of these probes, Stern–Volmer quenching constants, K_{SV} , for the steady-state fluorescence quenching were determined from the

variation of fluorescence intensity in the absence (I_0) and presence (I) of low concentrations, c , of 1-alkyl-3-methylpyridinium in ethanenitrile. In order to quantify the quenching effect of the monomer (preventing aggregation), we have chosen the short chain $[C_4\text{mpy}]\text{Cl}$ homologue to perform the experiments, and (for $c < 0.6$ mM) a linear Stern–Volmer plot, $(I_0/I) = 1 + cK_{SV}$, was obtained (Figure 2a). From the slopes of the Stern–Volmer plots, values of $K_{SV} = (0.3 \pm 0.04)$ and (0.07 ± 0.005) mM^{-1} for pyrene and anthracene, respectively, were obtained. For the quenching of an excited state, we have $K_{SV} = k_q\tau_0$,^{28,29} where τ_0 is the fluorescence lifetime of the excited state and k_q is the rate constant for bimolecular quenching. By taking as reasonable approximations the published values of τ_0 of pyrene and anthracene in polar aerated solvents, respectively 18.9 ns (19.0 ns without O_2) and 4.2 ns (5.3 ns without O_2),³⁰ we calculated the values of the bimolecular quenching constant $k_q(\text{pyrene}) = (1.58 \pm 0.23) \times 10^{10} \text{ L mol}^{-1} \text{ s}^{-1}$ and $k_q(\text{anthracene}) = (1.67 \pm 0.12) \times 10^{10} \text{ L mol}^{-1} \text{ s}^{-1}$. This demonstrates that within the experimental error, the quenching is diffusion controlled ($k_{\text{diff}} = 1.9 \times 10^{10} \text{ L mol}^{-1} \text{ s}^{-1}$). The quenching mechanism probably involves electron transfer, but this is out of the scope of the current work.

The fact that the $[C_n\text{mpy}]\text{Cl}$ family may act as fluorescence quenchers opens the possibility of determining CMCs by detecting the surfactant concentration for which the quenching deviates from the normal Stern–Volmer equation, that is, from a slope comparable to that which occurs in homogeneous media. The onset of micellization, defined as the CMC, can be recognized as a pronounced break-point in the dependence of I_0/I versus the concentration of $[C_n\text{mpy}]\text{Cl}$ in aqueous solution. Typical graphs of this type for $[C_n\text{mpy}]\text{Cl}$ ($n = 12, 14, 16$, or 18) in aqueous solution by using pyrene as a fluorescence probe are shown in Figure 2b. The values of CMCs for all systems are presented in Table 1. In order to apply this new method, it is necessary that the CMC of certain compound–quencher combinations is not greater than the concentration at which complete quenching of fluorescence probes occurs. It means that this method requires an appropriate match between the fluorescence probe and the quencher. One should note here the very good agreement between values determined by using distinct methodologies. Having a good agreement between this new method and two well-established methods for the onset of aggregation, surface tension and ^1H NMR (see next section), is important. This avoids potentially fallacious interpretations which are a common occurrence when novel methods are used without the proof of concept.

Self-Aggregation Assessment by ^1H NMR. ^1H NMR resonances for the protons of $[C_n\text{mpy}]\text{Cl}$ undergo reasonable shifts as a function of the $[C_n\text{mpy}]\text{Cl}$ concentration, namely, the protons of the ring and the protons of the terminal CH_3 group. Figure 3 shows the evolution of the chemical shifts (δ , ppm) in the ^1H NMR spectra for the protons of the terminal CH_3 group as a function of the reciprocal concentration (logarithmic scale) of $[C_n\text{mpy}]\text{Cl}$.

Once again, in agreement with the previous methodologies, the chemical shift shows a distinctive decrease for all $n > 12$, indicating the change in the environment for these molecules as a function of their concentration, related to the self-aggregation in small micellar-type aggregates.

Self-Aggregation for Other Types of Cationic Rings—Assessment by Surface Tension and Ab Initio Calculations. The influence of the type of ring in the cation on the aggregation behavior was also investigated. The underlying influence of this effect is very complex because head groups have opposing

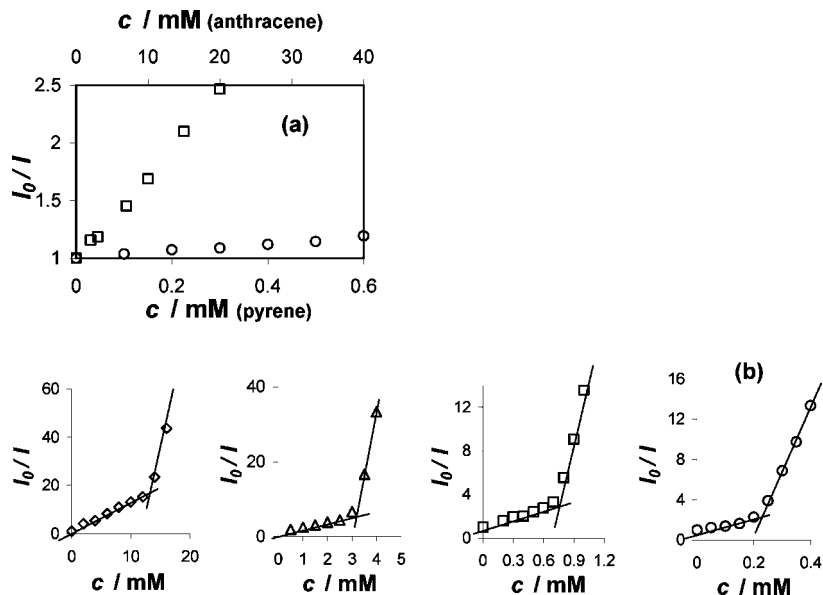


Figure 2. (a) Stern–Volmer relation for $[C_4\text{mpy}]\text{Cl}$ in ethanenitrile solutions of anthracene (\square) and pyrene (\circ). (b) Monitoring the self-aggregation of $[C_n\text{mpy}]\text{Cl}$ in aqueous solution by using the fluorescence quenching technique for pyrene for different alkyl side-chain lengths of the ionic liquid: $n = (\diamond)12$, $(\Delta)14$, $(\square)16$, and $(\circ)18$.

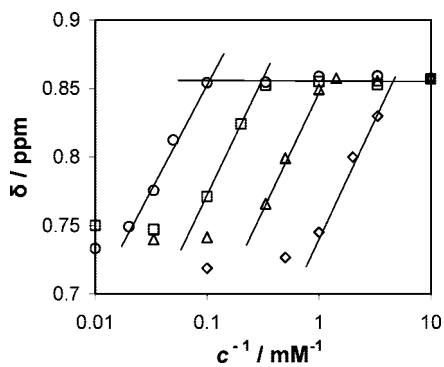


Figure 3. Monitoring the self-aggregation of $[C_n\text{mpy}]\text{Cl}$ by using ^1H NMR spectroscopy. δ is the observed chemical shift, and c is the ionic liquid concentration. Results for protons of the terminal CH_3 group for different chain lengths: $n = (\diamond)12$, $(\Delta)14$, $(\square)16$, and $(\circ)18$.

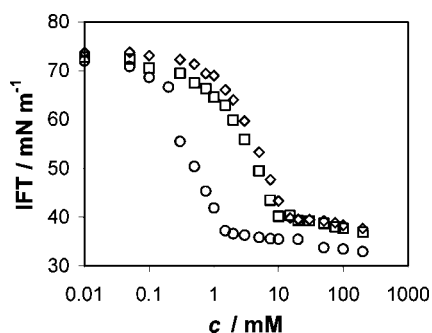


Figure 4. - Monitoring the self-aggregation of $[C_{12}\text{Y}]\text{Br}$ by using the IFT technique: $(\diamond)[C_{12}\text{mpip}]\text{Br}$, $(\square)[C_{12}\text{mpy}]\text{Br}$, and $(\circ)[C_{12}\text{mpyr}]\text{Br}$.

tendencies to keep close to minimize hydrocarbon–water contacts and to repel as a result of electrostatic repulsion, hydration, and steric hindrance.²⁵ Three ionic liquids with the same anion and the same alkyl chain length but with different types of hydrocarbon rings have been analyzed. Figure 4 shows the surface tension curves for $[C_{12}\text{Y}]\text{Br}$ ($\text{Y} = \text{mpyr}$, mpy , and mpip). Surprisingly, two very similar curves with almost the same CMC values were obtained for $[C_{12}\text{mpy}]\text{Br}$ and $[C_{12}\text{mpip}]\text{Br}$. Probably, in the case of $[C_{12}\text{mpip}]\text{Br}$, two effects

compensate each other. On the one hand, the higher hydrophobicity of the $[C_{12}\text{mpip}]^+$ cation and stronger bound anion, Br^- , in comparison with the $[C_{12}\text{mpy}]^+$ cation, where the positive charge is delocalized, would give a lower CMC. On the other hand, because these two molecules have a different geometry and volume, we can expect that the more space-demanding $[C_{12}\text{mpip}]^+$ cation (we are comparing boat and/or chair structures of a cyclic six-membered ring with a planar aromatic molecule) has a higher CMC because of steric hindrance. One can also notice that the CMC value for $[C_{12}\text{mpy}]\text{Br}$ (10 mM) is lower than that for $[C_{12}\text{mpy}]\text{Cl}$ (13 mM). The slightly lower values obtained for $[C_n\text{mpy}]\text{Br}$ are expected because it is known that the binding of anionic counterions to cationic micelles increases in the order $\text{F}^- < \text{Cl}^- < \text{Br}^- < \text{I}^-$.³¹

It is even more difficult to explain the significantly lower CMC and surface tension in the plateau region of the five-membered heterocyclic ring of $[C_{12}\text{mpyr}]\text{Br}$ in comparison with the six-membered heterocyclic ring of $[C_{12}\text{mpip}]\text{Br}$. Without further studies, we are unable to speculate whether this is only the effect of their different volume and geometry and consequent head packing in the micelles or in the monolayers. However, a complementary interpretation can be developed if one compares the geometry and internal charge distribution of the two isolated cations.

The necessary data were calculated *ab initio* (cf. Table S1 of the Supporting Information), and different conclusions can be drawn from. First, the geometry (bond lengths and angles) around the nitrogen atom are very similar in both cases ($\text{N}-\text{C}(\text{methyl})$ and $\text{N}-\text{C}(\text{methylene})$ distances of 149 and 151 pm, respectively, and angles close to 109.5°). This can be seen in Figure 5, where the most stable conformation of each cation is represented. In fact, the chair conformation of the piperidinium cation can be thought as an envelope conformation (like that of the pyrrolidinium cation) with an extra flap. Because that extra flap occupies a position opposite to the nitrogen atom, the influence of the former on the latter is very limited from a geometrical perspective. Also, the charge distribution in the two cations is quite different because of different hyper-conjugation effects on the five- and six-membered rings (cf. Figure 5).

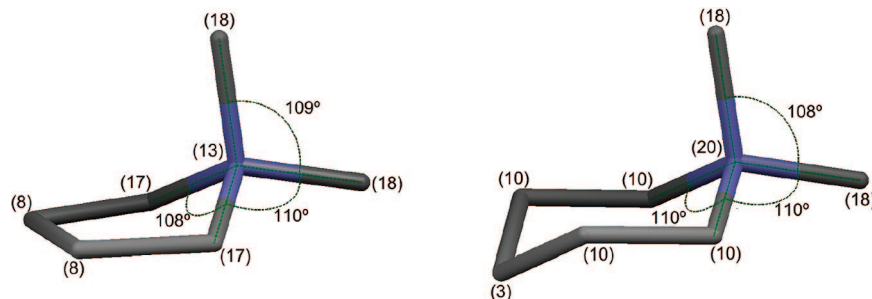


Figure 5. Most stable conformers of 1,1-dimethylpyrrolidinium (envelope conformation, left) and 1,1-dimethylpiperidinium (chair conformation, right). When a long alkyl chain is present, it will occupy an equatorial position relative to the pseudo-plane of the ring. The numbers in brackets are the point charges (in % acu) attributed by the model to the nitrogen, methylene, and methyl groups.

Taken together, these conclusions mean that the headgroup of the anion will interact with the two cations at a similar position (the most positive charge is centered around the geometrically similar nitrogen atoms) but with different magnitude. In fact, the larger charge density on the nitrogen of the piperidinium cation will lead to weaker interactions because this atom (surrounded by four carbon atoms) cannot be approached by the anion. On the other hand, the pyrrolidinium cation has greater charge densities in the 2,6-methylene groups (taken as the sum of the charge of the ortho carbon atom plus its two hydrogen atoms) where most of the interactions with the anion will take place. This fact can compensate for the lower charge density of its nitrogen atom and lead to an effectively higher counteranion binding, and consequently, to a lower CMC, as experimentally measured. These observations have to be examined in deeper detail by using other classes of ionic liquids and other methods.

4. Conclusions

We propose a novel methodology that can be used to find out whether ionic liquids are capable of forming aggregates in aqueous solutions. This technique is based on the fluorescence quenching effect that specific ionic liquids provoke in common fluorophores. This procedure was successfully tested against two well-established methodologies. Additional classes of ionic liquids can now be checked for their micellar behavior by using this new technique.

Quenching of fluorescence has found wide utility in biochemical research.²⁸ The current new result, connected to aggregation phenomena in ionic-liquids-containing systems, may find application in other fields too.

It was found that pyridinium ionic liquids are more biodegradable than imidazolium ionic liquids and biodegradation rates increase with longer alkyl chain length.³² The ability of pyridinium ionic liquids to act as a quencher for some fluorophores can be used as a very sensitive method for following their degradation rates or generally concentration change. This method can be used in broad concentration range and in the presence of many other species in solution, because quenching requires specific contact pyridinium nucleus–fluorophore.

Besides the length of the alkyl chain and the nature of the anion, both the structure of the headgroup and the point-charge density distribution are parameters which play important roles in the geometry and packing of micelles, in particular by controlling the magnitude of the steric repulsions between the head groups. However, the issue of the influence of the headgroup on the aggregation behavior deserves further investigations.

Acknowledgment. This work was supported by the Fundação para a Ciência e Tecnologia (FC&T), Portugal (Projects POCTI/

QUI/35413/2000 and POCI/QUI/57716/2004). M.B. thanks FC&T for a Ph.D. Grant SFRH/BD/13763/2003) and Marie Curie Fellowships for Early Stage Research Training (EST No505613). K.R.S. thanks the EPSRC (Portfolio Partnership Scheme, Grant no. EP/D029538/1).

Supporting Information Available: Experimental methods and detailed ab initio results. This material is available free of charge via the Internet at <http://pubs.acs.org>.

References and Notes

- (1) Rebelo, L. P. N.; Canongia Lopes, J. N.; Esperança, J. M. S. S.; Guedes, H. J. R.; Łachwa, J.; Najdanovic-Visak, V.; Visak, Z. P. *Acc. Chem. Res.* **2007**, *40*, 1114.
- (2) Bowers, J.; Butts, C. P.; Martin, P. J.; Vergara-Gutierrez, M. C.; Heenan, R. K. *Langmuir* **2004**, *20*, 2191.
- (3) Blesic, M.; Marques, M. H.; Plechkova, N. V.; Seddon, K. R.; Rebelo, L. P. N.; Lopes, A. *Green Chem.* **2007**, *9*, 481.
- (4) Blesic, M.; Gunaratne, N.; Lopes, A.; Plechkova, N. V.; Rebelo, L. P. N.; Seddon, K. R. In *Ionic Liquids: Never the Twain*; Gaune-Escard, M., Seddon, K. R., Eds.; Wiley: Hoboken, NJ, 2008. In preparation.
- (5) Sirieix-Plénet, J.; Gaillon, L.; Letellier, P. *Talanta* **2004**, *63*, 979.
- (6) Miskolczy, Z.; Sebök-Nagy, K.; Biczók, L.; Göktürk, S. *Chem. Phys. Lett.* **2004**, *400*, 296.
- (7) Vanyúr, R.; Biczók, L.; Miskolczy, Z. *Colloid Surf., A* **2007**, *299*, 25.
- (8) Goodchild, I.; Collier, L.; Millar, S. L.; Prokeš, I.; Lord, J. C. D.; Butts, C. P.; Bowers, J.; Webster, J. R. P.; Heenan, R. K. *J. Colloid Interface Sci.* **2007**, *307*, 455.
- (9) Wang, J.; Wang, H.; Zhang, S.; Zhang, H.; Zhao, Y. *J. Phys. Chem. B* **2007**, *111*, 6181.
- (10) Modarelli, A.; Sifaoui, H.; Mielcarz, M.; Domańska, U.; Rogalski, M. *Colloid Surf., A* **2007**, *302*, 181.
- (11) Dong, B.; Li, N.; Zheng, L.; Yu, L.; Inoue, T. *Langmuir* **2007**, *23*, 4178.
- (12) Singh, T.; Kumar, A. *J. Phys. Chem. B* **2007**, *111*, 7843.
- (13) El Seoud, O. A.; Pires, P. A. R.; Abdel-Moghny, T.; Bastos, E. L. *J. Colloid Interface Sci.* **2007**, *313*, 296.
- (14) (a) Najdanovic-Visak, V.; Canongia Lopes, J. N.; Visak, Z. P.; Trindade, J.; Rebelo, L. P. N. *Int. J. Mol. Sci.* **2007**, *8*, 736. (b) Lopes, J. N. C.; Rebelo, L. P. N. *Chimica Oggi/Chem. Today* **2007**, *25*, 37.
- (15) Anderson, J. L.; Pino, V.; Hagberg, E. C.; Sheares, V. V.; Armstrong, D. W. *Chem. Comm.* **2003**, *19*, 2444.
- (16) Fletcher, K. A.; Pandey, S. *Langmuir* **2004**, *20*, 33.
- (17) He, Y.; Li, Z.; Simone, P.; Lodge, T. P. *J. Am. Chem. Soc.* **2006**, *128*, 2745.
- (18) Thomaier, S.; Kunz, W. *J. Mol. Liq.* **2007**, *130*, 104.
- (19) Velasco, S. B.; Turmine, M.; Di Caprio, D.; Letellier, P. *Colloid Surf., A* **2006**, *275*, 50.
- (20) (a) Mandal, P. K.; Samanta, A. *J. Phys. Chem. B* **2005**, *109*, 15172. (b) Paul, A.; Mandal, P. K.; Samanta, A. *J. Phys. Chem. B* **2005**, *109*, 9148.
- (21) Blesic, M.; Plechkova, N. V.; Rebelo, L. P. N.; Seddon, K. R. *J. Mater. Chem.* To be submitted.
- (22) Frisch, M. J.; Trucks, G. W.; Schlegel, H. B.; Scuseria, G. E.; Robb, M. A.; Cheeseman, J. R.; Montgomery, J. A., Jr.; Vreven, T.; Kudin, K. N.; Burant, J. C.; Millam, J. M.; Iyengar, S. S.; Tomasi, J.; Barone, V.; Mennucci, B.; Cossi, M.; Scalmani, G.; Rega, N.; Petersson, G. A.; Nakatsuji, H.; Hada, M.; Ehara, M.; Toyota, K.; Fukuda, R.; Hasegawa, J.; Ishida, M.; Nakajima, T.; Honda, Y.; Kitao, O.; Nakai, H.; Klene, M.; Li, X.; Knox, J. E.; Hratchian, H. P.; Cross, J. B.; Bakken, V.; Adamo, C.; Jaramillo, J.; Gomperts, R.; Stratmann, R. E.; Yazyev, O.; Austin, A. J.; Cammi, R.; Pomelli, C.; Ochterski, J. W.; Ayala, P. Y.; Morokuma, K.

Voth, G. A.; Salvador, P.; Dannenberg, J. J.; Zakrzewski, V. G.; Dapprich, S.; Daniels, A. D.; Strain, M. C.; Farkas, O.; Malick, D. K.; Rabuck, A. D.; Raghavachari, K.; Foresman, J. B.; Ortiz, J. V.; Cui, Q.; Baboul, A. G.; Clifford, S.; Cioslowski, J.; Stefanov, B. B.; Liu, G.; Liashenko, A.; Piskorz, P.; Komaromi, I.; Martin, R. L.; Fox, D. J.; Keith, T.; Al-Laham, M. A.; Peng, C. Y.; Nanayakkara, A.; Challacombe, M.; Gill, P. M. W.; Johnson, B.; Chen, W.; Wong, M. W.; Gonzalez, C.; Pople, J. A. *Gaussian 03*, revision B.04; Gaussian, Inc.: Wallingford, CT, 2003.

(23) Canongia Lopes, J. N.; Deschamps, J.; Padua, A. A. H. *J. Phys. Chem. B* **2004**, 108, 2038.

(24) Rosen, M. J. *Surfactant and Interfacial Phenomena*; Wiley-Interscience, John Wiley & Sons: NJ, 2004.

(25) Evans, D. F.; Wennerstrom, H. *The Colloidal Domain: Where Physics, Chemistry, Biology and Technology Meet*; VCH: New York, 1994.

(26) Zana, R. *Surfactant Solutions: New Methods of Investigation*, Marcel Dekker: New York, 1986.

(27) Aguiar, J.; Carpena, P.; Molina-Bolívar, J. A.; Carnero Ruiz, C. *J. Colloid Interface Sci.* **2003**, 258, 116.

(28) Lackowicz, J. *Principles of Fluorescence Spectroscopy*; Plenum Press: New York, 1983.

(29) Birks, J. B. *Photophysics of Aromatic Molecules*; Wiley-Interscience: London, 1970.

(30) Murov, S. L.; Carmichael, I.; Hug, G. L. *Handbook of Photochemistry*, 2nd ed.; Marcel Dekker: New York, 1993.

(31) Anacker, E. W.; Ghose, H. M. *J. Am. Chem. Soc.* **1968**, 90, 3161.

(32) Docherty, K. M.; Dixon, J. K.; Kulpa, C. F., Jr *Biodegradation* **2007**, 18, 481.

JP802179J